Initiation of excitation fronts and related problems

VNB, II, BB, RDS

March 24, 2015

Contents and Plan of work

Part I
McKean model fronts – Example of a critical nucleus (standing wave)

1 Introduction

We apply the approach of Idris and Biktashev [7] for determining the conditions for initiation of excitation of propagating fronts in excitable media to the McKean model [9]. This exercise serves several purposes as detailed below.

- Exact analytical solutions can be found for the McKean model. The analytical expressions allow to validate and estimate the accuracy of the initiation criteria derived and the numerical procedures proposed. Such a benchmark is valuable because more "realistic" models such as those of cardiac excitability are only solvable numerically.
- The McKean model has piecewise smooth kinetics similar to "realistic" cardiac models. In contrast, the popular choice of a simplified model, the Zeldovich-Frank-Kamenetsky equation has smooth right-hand side.

We consider the following problem for a propagating excitation front formulated in terms of the McKean equation

$$\begin{aligned}
&\frac{\partial u}{\partial t} = \frac{\partial^2 u}{\partial x^2} + g(u) + H(x,t), \qquad g(u) = -u + \theta(u-a), \quad a \in (0,1/2),\\
&u(x,0) = u_0(x),\\
&\left[\frac{\partial u}{\partial x}\right]_{x=0} = 0, \qquad \lim_{x\to\infty} |u| < \infty,\\
&\quad x,t \in [0,\infty),
\end{aligned} \tag{1}$$

where $H(x,t)$ is an external stimulus current, $\delta(x)$ and $\theta(x)$ are the Dirac δ–function and the Heaviside step function, respectively.

2 The critical nucleus of the McKean model

Definition 1. *The steady-state (time-independent) solution of a problem of the type* (1) *is called a* critical nucleus.

So in this section we solve the ODE boundary value problem (BVP) given by

$$\begin{aligned}
&0 = \frac{\partial^2 u}{\partial x^2} - u + \theta(u-a), \qquad a \in (0,1/2), \qquad x \in [0,\infty),\\
&\left[\frac{\partial u}{\partial x}\right]_{x=0} = 0, \qquad \lim_{x\to\infty} |u| < \infty.
\end{aligned} \tag{2}$$

2.1 Exact analytical solution

2.1.1 Partitioning

Partition the domain of integration $x \in [0,\infty) = [0,\xi] \cup [\xi,\infty)$. Denote all quantities on interval $[0,\xi]$ by index $(_{:1})$ and quantities on interval $[\xi,\infty)$ by index $(_{:2})$. On the two intervals equations (2) take the form

$$\begin{aligned} &x_{:1} \in [0,\xi], \\ &{u_{:1}}'' - u_{:1} = 1, \\ &{u_{:1}}'(0) = 0, \\ &u_{:1}(\xi) = a, \end{aligned} \tag{3}$$

$$\begin{aligned} &x_{:2} \in [\xi,\infty), \\ &{u_{:2}}'' - u_{:2} = 0, \\ &u_{:2}(\xi) = a, \\ &\lim_{x_{:2}\to\infty} |u_{:2}| < \infty, \end{aligned} \tag{4}$$

$${u_{:1}}'(\xi) = {u_{:2}}'(\xi). \tag{5}$$

The partitioning introduces the internal matching point ξ as an additional unknown. To find ξ we require an extra condition – we assume that the solution is differentiable, hence (5).

2.1.2 Solution

The general solution of equations (3,4,5) is

$$\begin{aligned} &x_{:1} \in [0,\xi], \\ &u_{:1}(x_{:1}) = A_{:1}e^{x_{:1}} + B_{:1}e^{-x_{:1}} + 1, \end{aligned} \qquad \begin{aligned} &x_{:2} \in [\xi,\infty), \\ &u_{:2}(x_{:2}) = A_{:2}e^{x_{:2}} + B_{:2}e^{-x_{:2}}. \end{aligned}$$

The boundary conditions and the constraint give the equations

$$\begin{aligned} &A_{:1} - B_{:1} = 0, \\ &A_{:1}e^{\xi} + B_{:1}e^{-\xi} + 1 = a, \\ &A_{:2}e^{\xi} + B_{:2}e^{-\xi} = a, \\ &A_{:2} = 0, \\ &A_{:1} = A_{:2}, \end{aligned}$$

which we solve to find

$$A_{:1} = B_{:1} = \frac{a-1}{2\cosh\xi}, \quad A_{:2} = 0, \quad B_{:2} = ae^{\xi}, \quad \xi = -\frac{1}{2}\log(1-2a).$$

In summary, the critical nucleus is

$$u(x) = \begin{cases} u_{:1}(x) = 1 + \dfrac{a-1}{\cosh\xi}\cosh x = 1 - e^{-\xi}\cosh(x) = 1 - \sqrt{1-2a}\cosh x & \text{if } x \le \xi, \\ u_{:2}(x) = ae^{\xi-x} = \dfrac{a}{\sqrt{1-2a}}\mathrm{e}^{-x} & \text{if } x \ge \xi. \end{cases} \tag{6}$$

2.2 Accurate numerical solution

The numerical solution can be found using the same idea. But a suitable numerical formulation requires several modifications and additions as follows.

(a) The infinite domain of integration $x \in [0,\infty)$ be replaced by a finite interval, (see section 2.2.2).

(b) Equations (3) and (4) be posed on the same interval so that they can be solved as one system of coupled equations (see section 2.2.3).

(c) The equations are formulated as a first-order system since standard BVP routines often require that (see section 2.2.1).

2.2.1 Rewrite as first-order systems

We rewrite equations (3,4,5) by defining an auxiliary variable to represent the first derivative. We have

$$
\begin{aligned}
&x_{:1} \in [0,\xi], \\
&u_{:1}{}' = v_{:1}, \\
&v_{:1}{}' = u_{:1} - 1, \\
&v_{:1}(0) = 0, \\
&u_{:1}(\xi) = a,
\end{aligned}
\tag{7}
$$

$$
\begin{aligned}
&x_{:2} \in [\xi,\infty), \\
&u_{:2}{}' = v_{:2}, \\
&v_{:2}{}' = u_{:2}, \\
&u_{:2}(\xi) = a, \\
&\lim_{x_{:2}\to\infty} |u_{:2}| < \infty,
\end{aligned}
\tag{8}
$$

$$
v_{:1}(\xi) = v_{:2}(\xi). \tag{9}
$$

2.2.2 Replace the infinite domain of integration by finite

We need to replace the infinite interval $[0,\infty)$ by a finite interval $[0,L]$. To do this we need to replace the boundary condition at infinity by a condition at L. We assume that as $x \to \infty$ the solution approaches an equilibrium state. So we (a) find the equilibrium states of the McKean equation (1), (b) assume that at the right end of a finite domain of integration the solution is a small deviation from that equilibrium. In other words, we linearise as follows.

Consider $x > \xi$, then the McKean equation (1) is

$$
\frac{\partial u_{:2}}{\partial t} = \frac{\partial^2 u_{:2}}{\partial {x_{:2}}^2} - u_{:2}.
$$

The unique equilibrium solution, obtained at vanishing derivatives, is

$$
u_{:2} = 0.
$$

The time-independent McKean equation linearised near that state is

$$
\frac{\partial^2 \tilde{u_{:2}}}{\partial {x_{:2}}^2} - \tilde{u_{:2}} = 0,
$$

with solution and its derivative

$$
\tilde{u_{:2}}(x) = Ae^{x_{:2}} + Be^{-x_{:2}}, \qquad \tilde{u_{:2}}{}'(x) = Ae^{x_{:2}} - Be^{-x_{:2}},
$$

respectively. Reject the $\exp(x_{:2})$ term as unbounded and eliminate the unknown constant B by taking the ratio

$$
\frac{\tilde{u_{:2}}(x)}{\tilde{u_{:2}}{}'(x)} = \frac{Be^{-x_{:2}}}{-Be^{-x_{:2}}} = -1.
$$

We can now use this relationship as a boundary condition at the right end of the domain of integration

$$
u_{:2}(L) = -{u_{:2}}'(L) \qquad \text{or} \qquad u_{:2}(L) = -v_{:2}(L). \tag{10}
$$

Without loss of generality, we select $L = \xi + l$.

2.2.3 Map the domains of integration to [0,1]

We define the following maps and find the following derivative transformations

$$
x_{:1} \in [0,\xi] \to [0,1] \ni \underset{\sim}{x} \quad \text{by} \quad \underset{\sim}{x} = x_{:1}/\xi \qquad \Rightarrow \qquad \frac{\partial}{\partial x_{:1}} = \frac{1}{\xi}\frac{\partial}{\partial \underset{\sim}{x}}, \tag{11a}
$$

$$
x_{:2} \in [\xi,\xi+l] \to [0,1] \ni \underset{\sim}{x} \quad \text{by} \quad \underset{\sim}{x} = (x_{:2}-\xi)/l \qquad \Rightarrow \qquad \frac{\partial}{\partial x_{:2}} = \frac{1}{l}\frac{\partial}{\partial \underset{\sim}{x}}. \tag{11b}
$$

2.2.4 Numerical formulation and solution

/rswork1/02_Papers_Proposals/017_InitiationofExcitation/02Calcs/02McKean/01CriticalNucleus/Numerical/2013-12-01

Using change of variables (11) and the boundary condition (10), equations (7,8,9) take a form suitable for solution by standard numerical packages such as MAPLE or MATLAB,

$$
\begin{aligned}
&{u_{:1}}' = \xi v_{:1}, \quad {v_{:1}}' = \xi(u_{:1}-1), \quad {u_{:2}}' = l v_{:2}, \quad {v_{:2}}' = l u_{:2}, \\
&v_{:1}(0) = 0, \quad u_{:1}(1) = a, \quad u_{:2}(0) = a, \quad v_{:2}(1) = -u_{:2}(1), \quad v_{:1}(1) = v_{:2}(0), \\
&\underset{\sim}{x} \in [0,1],
\end{aligned}
\tag{12}
$$

where primes $(')$ denote derivatives wrt $\underset{\sim}{x}$.

In MAPLE this is implemented directly “as is”.

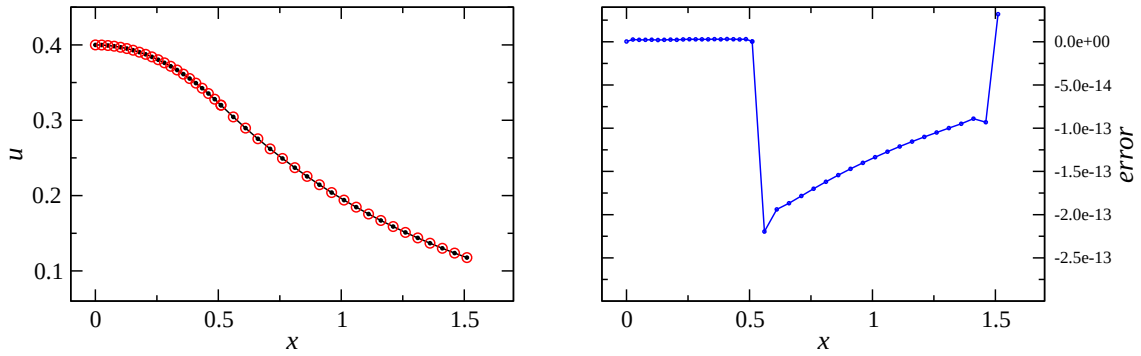

Figure 1: Numerical solution Num$[u(x)]$ and exact analytical solution $u(x)$ given by (6) for the critical nucleus of the McKean front equation at $a = 0.32$. The left panel shows the numerical solution Num$[u(x)]$ as a black line with small circles and the exact analytical solution $u(x)$ as larger red circles. The right panel shows the numerical error $u(x) - \text{Num}[u(x)]$.

```
######################################################################
# Critical nucleus

NumbEqus:=4:
NumbBCs:=5:  # + 1 unknown param

#...The Equations that we need to solve, formulated as a first order system
#-----------------------------1--------------------------
 F[1] := diff(u1(x),x) = xa* v1(x):
 F[2] := diff(v1(x),x) = xa*(u1(x)-1):
#-----------------------------2--------------------------
 F[3] := diff(u2(x),x) = l*v2(x):
 F[4] := diff(v2(x),x) = l*u2(x):
#------------------------------------------------------

#The boundary conditions in the format of the D02RAF are
 AL[1] := u1(1) = a:
 AL[2] := v1(0) = 0:
 AL[3] := u2(0) = a:
 AL[4] := v2(1) = -u2(1):
 AL[5] := v1(1) = v2(0):

PROBLEM:={seq(F[i],i=1..NumbEqus), seq(AL[i],i=1..NumbBCs)}:
VARS:=[u1(x), u2(x), v1(x), v2(x)]:
######################################################################
```

The equations are then solved using the MAPLE `dsolve,numeric` command.

```
Y:= dsolve(PROBLEM,numeric,
          VARS,
          method=bvp[middefer],'range'=0..1,maxmesh=8192,'abserr'=Float(1,-10),
          'optimize'=true,'output'=listprocedure):
```

Comparison of the numerical solution Num$[u(x)]$ and the exact analytical solution $u(x)$ given by (6) for the critical nucleus of the McKean model are shown in figures 1 and (**??**). The numerical solution is very accurate.

3 Linearization about the critical nucleus

3.1 Exact analytical solution

3.1.1 Linearisation and Separation of variables

In this section we denote the critical nucleus (6) by $u_*(x)$. We consider small perturbations about the critical nucleus

$$u(x,t) = u_*(x) + \tilde{u}(x,t), \qquad \tilde{u}(x,t) \ll 1.$$

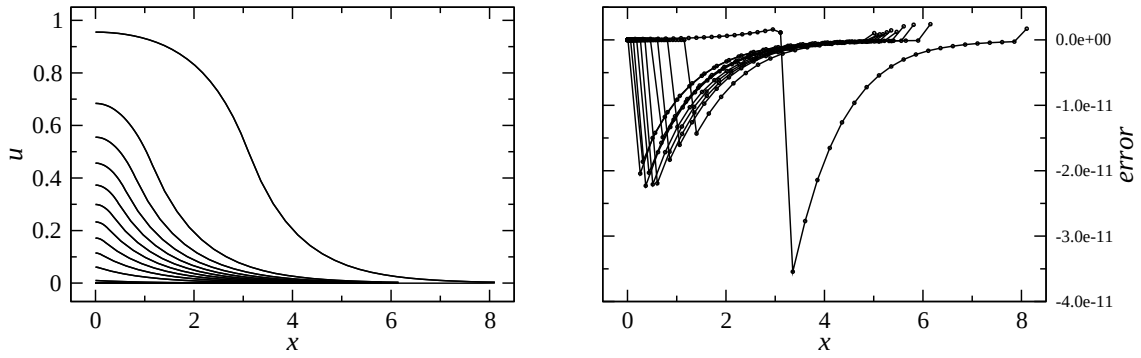

Figure 2: Same as figure 1 but with values of $a = 0.01$, 0.0589, 0.1078, 0.1567, 0.2056, 0.2545, 0.3034, 0.3523, 0.4012, 0.4501, 0.499 increasing from top to bottom in the left panel.

Linearising equations (1) near the critical nucleus we obtain

$$\begin{aligned}
&\frac{\partial \tilde{u}}{\partial t} = \frac{\partial^2 \tilde{u}}{\partial x^2} + g'(u_*)\tilde{u}, \qquad g'(u_*) = \left[\frac{\partial}{\partial \tilde{u}} g(u)\right]_{u=u_*} = -1 + a^{-1}\delta(x-\xi),\\
&\tilde{u}(x,0) = \tilde{u}_0(x),\\
&\left[\frac{\partial \tilde{u}}{\partial x}\right]_{x=0} = 0, \qquad \lim_{x\to\infty} \tilde{u} = 0,\\
&\quad x, t \in [0,\infty).
\end{aligned} \tag{13}$$

By separation of variables we find that $\tilde{u}(x,t)$ can be represented as

$$\tilde{u}(x,t) = e^{\lambda t}\phi(x),$$

where the eigenpair $(\lambda, \phi(x))$ satisfy the Sturm-Liouville eigenvalue problem

$$\begin{aligned}
&\phi'' + a^{-1}\delta(x-\xi)\phi = \mu^2\phi, \qquad \mu^2 = \lambda + 1\\
&\phi'(0) = 0, \qquad \lim_{x\to\infty} \phi = 0.
\end{aligned} \tag{14}$$

Aside. The derivative of the Heaviside function needed for $g'(u_*)$ is

$$\left[\frac{\partial}{\partial u}\theta(u(x)-a)\right]_{u=u_*} = \delta\big(u_*(x)-a\big) = \frac{\delta\big(\xi-x\big)}{\big|\big(u_*(\xi)-a\big)'\big|} = \frac{\delta\big(\xi-x\big)}{|u_*'(\xi)|} = \frac{\delta\big(\xi-x\big)}{a}.$$

Here we use the well-known formula for a composition with a δ-function,

$$\delta \circ \varphi(x) = \delta\big(\varphi(x)\big) = \sum_i \frac{\delta\big(x-x_i\big)}{|\varphi'(x_i)|},$$

where x_i are the roots of the equation $\varphi(x) = 0$. In our case $\varphi(x) = u_*(x) - a$ with a unique root $x = \xi$.

3.1.2 Partitioning and solution

To take care of the δ-function, we partition the domain of integration $x \in [0,\infty) = [0,\xi] \cup [\xi,\infty)$. Denote all quantities on interval $[0,\xi]$ by index $(_{:1})$ and quantities on interval $[\xi,\infty)$ by index $(_{:2})$. On the two intervals equations (14) take the form

$$\begin{aligned}
&x_{:1} \in [0,\xi],\\
&\phi_{:1}'' = \mu^2\phi_{:1},\\
&\phi_{:1}'(0) = 0,
\end{aligned} \tag{15}$$

$$\begin{aligned}
&x_{:2} \in [\xi,\infty),\\
&\phi_{:2}'' = \mu^2\phi_{:2},\\
&\lim_{x\to\infty} \phi_{:2} = 0,
\end{aligned} \tag{16}$$

$$\begin{aligned}
&\phi_{:1}(\xi) = \phi_{:2}(\xi),\\
&\phi_{:2}'(\xi) - \phi_{:1}'(\xi) + a^{-1}\phi_{:1}(\xi) = 0.
\end{aligned} \tag{17}$$

The second of the matching conditions (17) is obtained in the standard way by integrating equation (14) from $\xi - \epsilon$ to $\xi + \epsilon$ and taking $\epsilon \to 0$.

The general solution of these linear equations is

$$\begin{aligned} &x_{:1} \in [0, \xi], && x_{:2} \in [\xi, \infty), \\ &\phi_{:1}(x_{:1}) = A_{:1} e^{\mu x_{:1}} + B_{:1} e^{-\mu x_{:1}}, && \phi_{:2}(x_{:2}) = A_{:2} e^{\mu x_{:2}} + B_{:2} e^{-\mu x_{:2}}. \end{aligned}$$

Imposing the boundary and matching conditions we find

$$\begin{aligned} &A_{:1} = B_{:1} = \frac{B_{:2}}{2} \frac{e^{-\mu\xi}}{\cosh(\mu\xi)}, \quad A_{:2} = 0, \quad B_{:2} = \text{left arbitrary}, \\ &\nu(1 + \tanh\nu) = \xi/a, \quad \nu = \mu\xi. \end{aligned} \tag{18}$$

The last equation is a characteristic equation giving the eigenvalues of the problem. It can be solved exactly, and after transforming $\nu \to \mu \to \lambda$, we obtain the following explicit exact expression for the first eigenvalue

$$\lambda_1 = \left[\left(a\, W_0 \left(\frac{\xi}{a} \exp\left(-\frac{\xi}{a} \right) \right) + \xi \right) \Big/ (2a\xi) \right]^2 - 1; \tag{19}$$

where $W_0(\cdot)$ is principal branch of the Lambert W-function as defined in [5]. The corresponding unstable first eigenfunction is

$$\phi_1(x) = \begin{cases} \cosh(\sqrt{\lambda_1 + 1}\, x), & x \in [0, \xi] \\ \cosh(\sqrt{\lambda_1 + 1}\, \xi)\, \exp(\sqrt{\lambda_1 + 1}\, (\xi - x)), & x \in [\xi, \infty), \end{cases} \tag{20}$$

where the arbitrary constant is set to $B_{:2} = e^{\mu\xi} \cosh(\mu\xi)$.

3.2 Accurate numerical solution

/rswork1/02_Papers_Proposals/017_InitiationofExcitation/02Calcs/02McKean/02LinearizationAndEigenvlues/02Numerical/2013-12-07/Equations.M
/rswork1/02_Papers_Proposals/017_InitiationofExcitation/02Calcs/02McKean/02LinearizationAndEigenvlues/02Numerical/2013-12-07/03_McKean_1stEigenvalue.M

3.2.1 Comments on straightforward generic approaches

There are a number of ways to solve the Sturm-Liouville eigenvalue problem (14) numerically[1] [11, 12]. One can attempt to solve the BVP (14) directly, that is without taking advantage of the known internal matching point at $x = \xi$. Two generic approaches to the numerical approximation of eigenvalues of a boundary value problem are

(a) Discretization. Finding eigenpairs by discretization can be done using standard finite-differences or finite-elements. When the a linear ODE problem $\mathcal{L}y = \lambda y$ is discretized by e.g. finite-differences one obtains an algebraic matrix eigenvalue problem $\boldsymbol{A} \cdot \boldsymbol{y} = \lambda \boldsymbol{y}$ that can be solved with any matrix eigenvalue solver for the matrix $\boldsymbol{A}$. The number of eigenpairs found is equal to the resolution used and the accuracy quickly deteriorates for the higher eigenpairs. Since our problem (14) involves a δ-function, a finite-element discretization will be more appropriate as the δ-function can be integrated-out when computing the projection integral. Burhan has used a FEM approach already.

(b) Shooting. Shooting methods are more accurate and require less storage and arithmetic. But they determine one eigenvalue at a time and usually they do not determine the index of the eigenvalue. For Sturm-Liouville problems, these difficulties are avoided by the Prüfer method, which is a shooting method based on oscillation. A Prüfer method is implemented in the SLEIGN2 code[2] [1] and in the NAG library code[3] D02KDF [10]. The Prüfer shooting methods have, however, some problems with stiffness when standard initial value solvers are used. This stiffness disappears when the Prüfer transformation is combined with coefficient approximation as implemented in the packages SLEDGE[4] and SL02F [8].

[1] http://gams.nist.gov/cgi-bin/serve.cgi/Class/I1b3
[2] http://www.math.niu.edu/SL2/
[3] http://www.nag.co.uk/numeric/fl/fldocumentation.asp
[4] http://www.netlib.org/misc/sledge

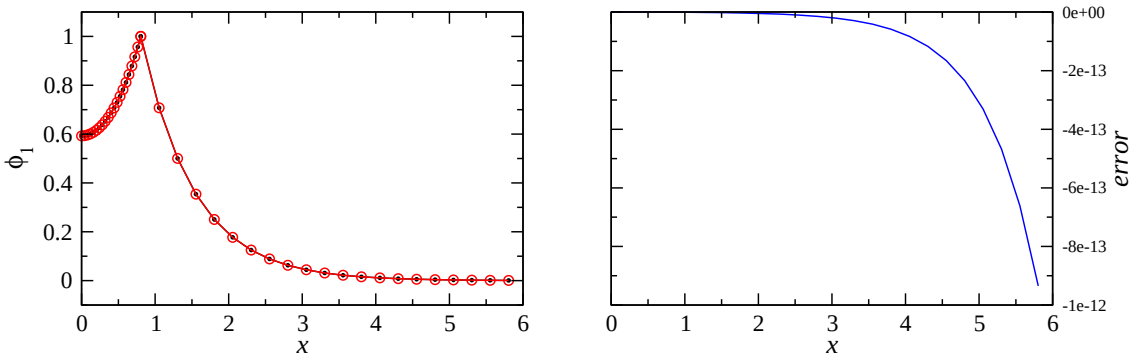

Figure 3: Numerical solution Num$[\phi_1(x)]$ and exact analytical solution $\phi_1(x)$ given by (20) for the first eigenfunction of the critical nucleus of the McKean front equation at $a = 0.4$. The left panel shows the numerical solution Num$[\phi_1(x)]$ as a black line with small circles and the exact analytical solution $\phi_1(x)$ as larger red circles. The right panel shows the numerical error $\phi_1(x) - \text{Num}[\phi_1(x)]$.

3.2.2 An accurate problem-specific approach and solution

We take advantage of the known structure of the problem and we adopt a problem-specific approach. In particular, we solve numerically equations (15), (16) and (17). The numerical formulation of the eigenvalue problem requires the following additional "tricks".

(a) The infinite domain of integration $x \in [0, \infty)$ needs to be replaced by a finite interval, as in section 2.2.1.

(b) Equations (15) and (16) need to be posed on the same interval so that they can be solved as one system of coupled equations, as in section 2.2.3.

(c) The equations need to be formulated as a first-order system, as in section 2.2.1.

(d) In addition, any eigenvalue problem requires one additional arbitrary "normalizing" condition to be specified. In our case, this corresponds to fixing the parameter $B_{:2}$ that was left undetermined in (18). We set

$$\phi(1) = 1,$$

which corresponds to $B_{:2} = 1/\cosh(\xi\sqrt{\lambda_1 + 1})$.

(e) As previously, we use the MAPLE `dsolve,numeric` command. `dsolve,numeric` is a finite-difference scheme but it behaves similarly to a shooting method in that it only returns one eigenvalue. We have the freedom to specify which eigenvalue is of interest. This can be done by, e.g. providing an initial guess such as an eigenfunction that oscillates a given number of times. In our case, the desired eigenvalue is specified implicitly when deriving an approximation to the boundary condition at infinity: the BC that is specified at the right end of the finite numerical domain of integration is only true for $\lambda > 0$, and we know from [7] that there is only one such eigenvalue.

In summary, the numerical formulation we pose is given by,

$$\begin{aligned}
&\phi_{:1}{}' = \xi\varphi_{:1}, \quad \varphi_{:1}{}' = \xi\mu^2\phi_{:1}, \quad \phi_{:2}{}' = l\varphi_{:2}, \quad \varphi_{:2}{}' = l\mu^2\phi_{:2},\\
&\varphi_{:1}(0) = 0, \quad \phi_{:1}(1) = \phi_{:2}(0), \quad \phi_{:2}(1) = -\varphi_{:2}(1)/\mu,\\
&\qquad \varphi_{:2}(0) - \varphi_{:1}(1) + \phi_{:1}(1)/a = 0, \quad \phi_{:1}(0) = 1,\\
&\underset{\sim}{x} \in [0, 1],
\end{aligned} \tag{21}$$

where primes $(')$ denote derivatives wrt $\underset{\sim}{x}$.

In MAPLE this can be implemented directly as is. However, it is even better to combine equations (12) for the critical nucleus and equations (21) for the first eigenpair in one composite system of equations. This has the advantages that the basic state u_* and the matching point $x = \xi$ are determined simultaneously with the eigenpair avoiding the need to pass this data between codes/-subroutines, and the total error can be minimized over the linear and the nonlinear problem. The Maple code is

```
#####################################################################
# Composite problem - Critical nucleus & its 1st eigenmode
```

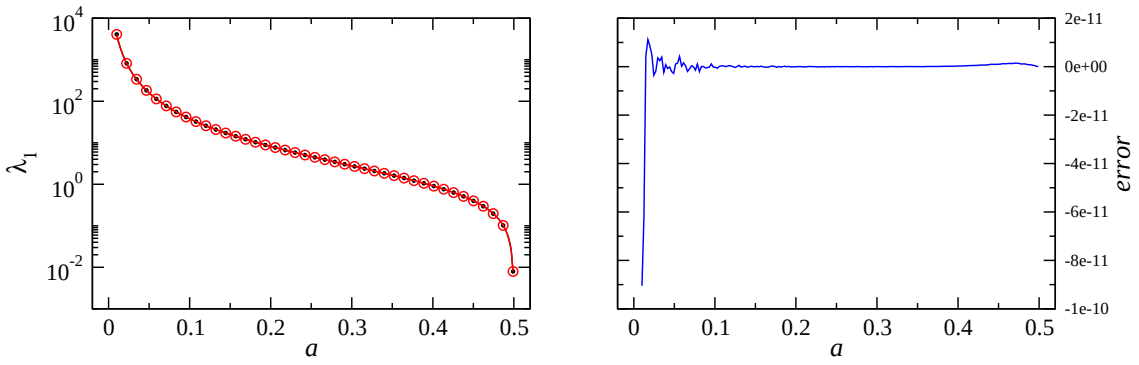

Figure 4: Numerical solution Num$[\lambda_1(a)]$ and exact analytical solution $\lambda_1(a)$ given by (19) for the first eigenvalue of the critical nucleus of the McKean front equation as a function of a. The left panel shows the numerical solution Num$[\lambda_1(a)]$ as a black line with small circles and the exact analytical solution $\lambda_1(a)$ as larger red circles. The right panel shows the numerical error $\lambda_1(a) - \text{Num}[\lambda_1(a)]$.

```
NumbEqus:=8:
NumbBCs:=10:

#...critical nucleus problem
#-----------------------------1--------------------------
 F[1] := diff(u1(x),x) = xa* v1(x):
 F[2] := diff(v1(x),x) = xa*(u1(x)-1):
#-----------------------------2--------------------------
 F[3] := diff(u2(x),x) = l*v2(x);
 F[4] := diff(v2(x),x) = l*u2(x);
#------------------------------------------------------

#The boundary conditions in the format of the D02RAF are
 AL[1] := u1(1) = a:
 AL[2] := v1(0) = 0:
 AL[3] := u2(0) = a:
 AL[4] := v2(1) = -u2(1):
 AL[5] := v1(1) = v2(0):

#...eigenvalue problem
#-----------------------------1--------------------------
 F[5] := diff(f1(x),x) = xa* ff1(x):
 F[6] := diff(ff1(x),x) = xa*mu^2*f1(x):
#-----------------------------2--------------------------
 F[7] := diff(f2(x),x) = l*ff2(x);
 F[8] := diff(ff2(x),x) = l*mu^2*f2(x);
#------------------------------------------------------

#The boundary conditions in the format of the D02RAF are
 AL[6] := f1(1) = 1:
 AL[7] := ff1(0) = 0:
 AL[8] := f1(1) = f2(0):
 AL[9] := mu*f2(1) = -ff2(1):
 AL[10]:= ff2(0) - ff1(1) +1/a*f1(1) = 0:

PROBLEM03:={seq(F[i],i=1..NumbEqus), seq(AL[i],i=1..NumbBCs)}:
VARS03:=[u1(x), u2(x), v1(x), v2(x), f1(x), f2(x), ff1(x), ff2(x)]:
#####################################################################
```

The equations are then solved using the MAPLE `dsolve,numeric` command.

```
Y:= dsolve(PROBLEM03,numeric,
          VARS03,
          method=bvp[middefer],'range'=0..1,maxmesh=8192,'abserr'=Float(1,-10),
          'optimize'=true,'output'=listprocedure):
```

Comparison of the numerical solution and the exact analytical solutions are shown in figure 3 and 4. The numerical solution is very accurate.

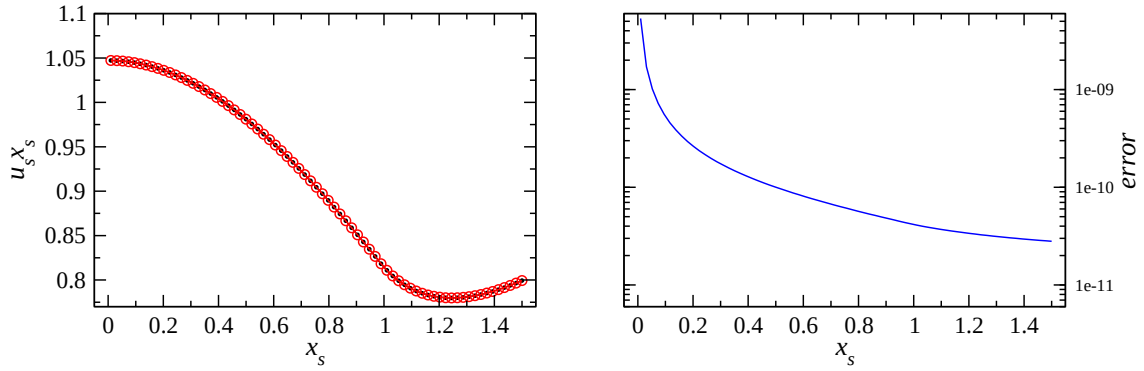

Figure 5: Numerical strength-extent curve Num$[u_s(x_s)]$ and the analytical approximation $u_s(x_s)$ given by formula (29) for the McKean front equation for $a = 0.43$. The left panel shows the numerical solution Num$[x_s u_s(x_s)]$ as a black line with small circles and the analytical approximation $x_s u_s(x_s)$ as larger red circles. The right panel shows the numerical error $u_s(x_s) -$ Num$[u_s(x_s)]$.

4 Initiation curves

Consider problem (1) with initial condition and with external forcing both in the form of rectangular impulses,

$$u_0(x) = u_s\theta(x_s - x), \tag{22}$$

$$H(x,t) = -2I_s\theta(t_s - t)\delta(x), \tag{23}$$

respectively.

Proposition 1. *The surface defined by the equation*

$$A_1(0) + 2\phi_1(0)\int_0^\infty \mathrm{e}^{-\lambda_1 t}\theta(t_s - t)\,\mathrm{d}t = 0, \tag{24}$$

where

$$A_j(0) = \int_{-\infty}^{\infty} \phi_j(x)\Big(u_0(x) - u_*(x)\Big)\,\mathrm{d}x, \tag{25}$$

is an approximation to the boundary in the $(x - t - u_s - I_s)$–space separating conditions leading to initiation from conditions leading to decay in the problem (1).

Derivation. See Idris and Biktashev [7]. □

We will consider two simpler special cases separately.

Initiation by initial conditions (by voltage) Consider problem (1) with no external forcing $H(x,t) = 0$ and with an initial condition in the form of a rectangular impulse (22).

Definition 2. *A curve in the $(x_s - u_s)$–plane that serves as a boundary between initial conditions leading to initiation and initial conditions leading to decay is called a* strength-extent curve.

Corollary 1. *The strength-extent curve for a problem of the type* (1) *is approximated by the equation*

$$\int_0^\infty \phi_1(x)\Big(u_s\theta(x_s - x) - u_*(x)\Big)\mathrm{d}x = 0. \tag{26}$$

Initiation by external stimulus Consider problem (1) with vanishing initial condition $u_0(t) = 0$ and with an external forcing in the form of a rectangular impulse (23).

Definition 3. *A curve in the $(t_s - I_s)$–plane that serves as a boundary between external forcing terms leading to initiation and external forcing terms leading to decay is called a* strength-duration curve.

Corollary 2. *The strength-duration curve for a problem of the type* (1) *is approximated by the equation*

$$-\int_{-\infty}^{\infty} \phi_1(x)u_*(x)\,\mathrm{d}x + 2I_s\phi_1(0)\int_0^\infty \mathrm{e}^{-\lambda_1 t}\theta(t_s - t)\mathrm{d}t = 0, \tag{27}$$

which can be solved to give

$$I_s(t_s) = \frac{\lambda_1\int_{-\infty}^{\infty}\phi_1(x)u_*(x)\,\mathrm{d}x}{2\phi_1(0)\big(1 - e^{-\lambda_1 t_s}\big)}. \tag{28}$$

4.1 Using proposed initiation criteria

In this subsection we evaluate expressions (26) and (27) analytically and numerically for the McKean equation.

4.1.1 Analytically

/rswork1/02_Papers_Proposals/017_InitiationofExcitation/02Calcs/02McKean/03EvaluateInitiation/01StrengthExtentCurve_Analytical.M
/rswork1/02_Papers_Proposals/017_InitiationofExcitation/02Calcs/02McKean/03EvaluateInitiation/11StrengthDurationCurve_Analytical.M

Substituting the expressions for the unstable first eigenpair (19), (20) and the critical nucleus (6) in equations (26) and (27) we obtain explicit approximations to the strength-extent and strength-duration curves. The integrals are straightforward to evaluate both analytically and numerically - they only need to be split taking into account the already known internal matching points.

Strength-extent curve. Solution of equation (26) in the case of the McKean equation gives

$$\widetilde{u_s} = \begin{cases} N/A & x_s \le \xi \\ N/B, & x_s \ge \xi, \end{cases} \tag{29}$$

where

$$N = \frac{a\cosh(\mu\xi)}{\mu+1} + \frac{\sinh(\mu\xi)}{\mu} - \frac{1}{2}\left(\frac{\sinh\left((\mu-1)\xi\right)}{\mu-1} + \frac{\sinh\left((\mu+1)\xi\right)}{\mu+1}\right)\mathrm{e}^{-\xi}, \tag{30}$$

$$A = \sinh(\mu x_s)/\mu,$$

$$B = e^{\mu\xi}\left(1 - e^{-\mu x_s}\cosh(\mu\xi)\right)/\mu.$$

The expression is illustrated in figure 5.

In the particular case of the McKean equation ignition is impossible for any $u_s < a$ as then the source term in the equation vanishes, $\theta(u_s - a)$=0. For this reason, equation (29) needs to be modified to

$$u_s = \max(\widetilde{u_s}, a).$$

According to (29) the expression $\widetilde{u_s}$ is monotonically decreasing function of x_s and so a unique solution of the equation $\widetilde{u_s}(x_{sa}) = a$ exists, namely

$$x_{sa} = \frac{1}{\mu}\left(\mu\xi + \log\left(\frac{a\cosh(\mu\xi)}{a\exp(\mu\xi) - N\mu}\right)\right). \tag{31}$$

With this the final explicit expression for the approximation to strength-extent curve in the McKean equation takes the form

$$u_s(x_s) = \begin{cases} N/A & x_s \in [0,\xi], \\ N/B, & x_s \in [\xi, x_{sa}], \\ a, & x_s \in [x_{sa}, \infty). \end{cases} \tag{32}$$

Comparison with DNS is described in the next subsection.

Strength-duration curve. The strength-duration curve is given by

$$I_s = N/C, \tag{33}$$

where

$$C = \left(1 - e^{\lambda_1 t_s}\right)/\lambda_1. \tag{34}$$

The expression is illustrated in figure 6.

4.1.2 Numerically

/rswork1/02_Papers_Proposals/017_InitiationofExcitation/02Calcs/02McKean/03EvaluateInitiation/05_McKean_StrengthExtent_Numerical.M
/rswork1/02_Papers_Proposals/017_InitiationofExcitation/02Calcs/02McKean/03EvaluateInitiation/15_McKean_StrengthDuration_Numerical.M

Once the critical nucleus and the first eigenpair have been computed numerically as detailed in the previous sections, the numerical evaluation of equations (32) and (33) is straightforward. The required integrals need to be split taking into account the already known internal matching points. See the Maple scripts listed above.

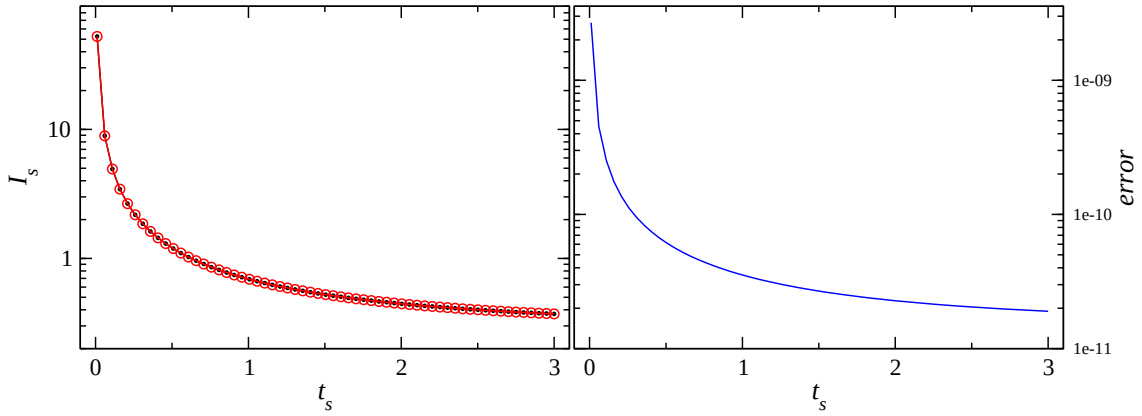

Figure 6: Numerical strength-duration curve Num$[I_s(t_s)]$ and the analytical approximation $I_s(t_s)$ given by formula (33) for the McKean front equation for $a = 0.43$. The left panel shows the numerical solution Num$[I_s(t_s)]$ as a black line with small circles and the analytical approximation $I_s(t_s)$ as larger red circles. The right panel shows the numerical error $I_s(t_s) -$ Num$[I_s(t_s)]$.

4.2 Using direct numerical simulations

/rswork1/02_Papers_Proposals/017_InitiationofExcitation/02Calcs/02McKean/04DNS/C/04

We now compare the explicit approximations for the strength-extent curve (32) and the strength-duration curve (33) to results obtained by direct numerical simulation of problem (1).

4.2.1 Numerical scheme

Schemes used. We tried a variety of numerical schemes to solve problem (1), including (a) first-order backward Euler step in time coupled to second-order finite-differences in space – absolutely stable and allows for large time-steps, implemented in MAPLE, (b) NAG subroutine `D03PPF` – a state-of-the-art scheme with adaptive time step and spatial remeshing, control of local and global errors, see NAG documentation, (c) MATLAB native PDE solver `pdepe`, (d) MAPLE native PDE solver `pdsolve,numeric`, (e) first-order forward Euler step in time coupled to second-order finite-differences in space. The results from these various schemes are essentially the same. Below we focus on the simplest scheme (e).

FTCS Scheme (e). The first-order forward Euler step in time coupled to second-order finite-differences in space is

$$
\begin{aligned}
x_k = kL/h_x, \quad t_j = jT/h_t, \qquad & (35)\\
u_k^0 = u_s\theta(x_s - x_k),\\
u_k^{j+1} = u_k^j + h_t(g(u_k^j) + (u_{k-1}^j - 2u_k^j + u_{k+1}^j)/h_x^2) + O(h_x^2, h_t^2), \qquad & k = 1\ldots K-1,\ j = 1\ldots J\\
u_0^{j+1} = (4u_1^j - u_2^j)/3 + O(h_x^3),\\
u_K^{j+1} = (4u_{N-1}^j - u_{N-2}^j)/3 + O(h_x^3),
\end{aligned}
$$

where L and T are finite space and time intervals, k and j are space and time and indices, h_x and h_t are space and time steps, respectively. The theoretical stability criterion for this scheme applied to a linear PDE is $h_t/h_x^2 < 1/2$, and our runs confirm that this estimate holds for our problem as well. We take advantage of this and fix the time step to

$$h_t = (4/9)h_x^2.$$

This is convenient as we now have a theoretical estimate of the local truncation error

$$O(h_x^2, h_t) = O(h_x^2),$$

and we can measure resolution by a single parameter, namely the space step h_x.

Bisection For a fixed set of parameter values $\{a, x_s, L, h_x\}$ the critical value of u_s that separates decay from ignition is found by bisection to a specified accuracy $\epsilon = 10^{-5}$. We use the criteria $\min_{x\in[0,L]} u(x) > a$ for ignition and $\max_{x\in[0,L]} u(x) < a$ for decay, respectively.

One version of the code is in

/rswork1/02_Papers_Proposals/017_InitiationofExcitation/02Calcs/02McKean/04DNS/C/04

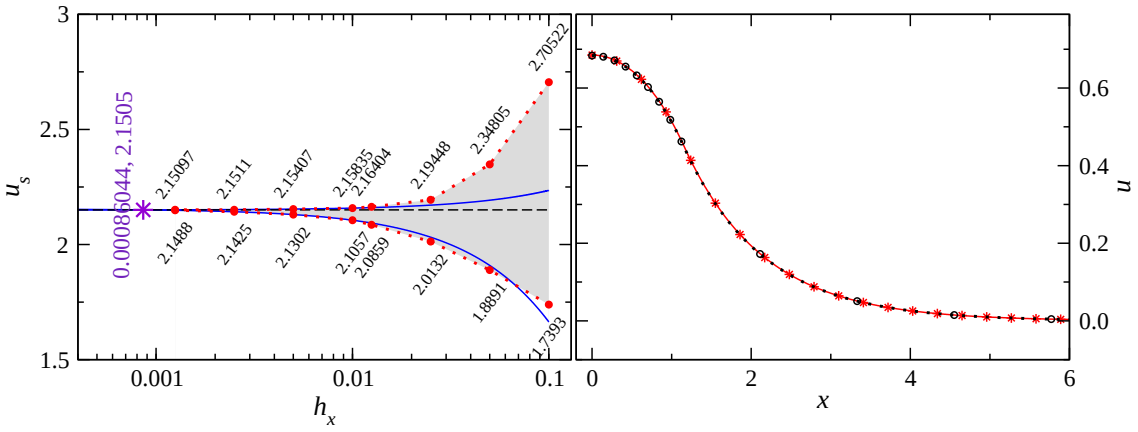

Figure 7: (a) The region where "frozen" solutions occur in direct numerical simulations for $a = 0.45$ and $x_s = 0.5$ and with variation of the space step h_x is located between the two dotted red lines with annotated data points and is shaded in gray. The thin solid blue lines are the lines of linear extrapolation (see section 4.2.2), the intersection of which gives the boundary between decay and ignition indicated by the violet star and annotated. (b) Comparison between the "frozen" solution obtained by direct numerical simulation at $a = 0.45$, $x_s = 0.5$, $u_s = 2.13$, $h_x = 0.01$ and the exact analytical expression for the critical nucleus (6) at $a = 0.45$.

4.2.2 Spurious "frozen" solutions

We found in section 3 that in the phase space of the McKean problem the critical nucleus solution u_* is a saddle point consisting of a stable manifold that is orthogonal to exactly one unstable direction with positive eigenpair $(\lambda_1, \phi_1(x))$. The stable manifold acts as a boundary between decay and ignition and stimuli of initial conditions can be parametrised by projection onto the unstable direction. For this reasons, we expect that any initial perturbation with amplitude u_s will either ignite or decay.

Problem. Contrary to this expectation for large values of a we encounter time-independent solutions in a finite range of u_s values. These "frozen" solutions are observed in all of the different numerical schemes we have tried (a-e, above). The "frozen" solutions appear to be identical to the corresponding critical nucleus (6) within the local truncation error as illustrated in figure 7(b). We have been unable to find a satisfying theoretical explanation of why frozen solutions exist. We suggest that the stability of the numerical scheme, e.g. the Forward-Time Central-Space scheme listed above (35) should be studied, but we were unable to complete the analysis due to the step function discontinuity. This problem will be deferred for future research.

We also remark that such problems with DNS serve as an additional motivation to develop theoretical ignition criteria.

Likely explanation. Our numerical experiments suggest that the "frozen" solutions are spurious and that their occurrence is due to limited accuracy of the numerical scheme insufficient to resolve the very slow evolution in the vicinity of the critical nucleus solution u_*. This problem is especially pronounced as a increases to 0.5 and the corresponding eigenvalue λ_1 decreases to asymptotically small values as illustrated in figure 3. Empirical evidence for this conclusion is presented in figure 7(a) where the region of "frozen" solutions is outlined as a function of the resolution h_x (i.e. as a function of the local truncation $O(h_x^2)$. Figure 7(a) shows that the region of "frozen" solutions shrinks and will eventually reduce to a single point as resolution is increased.

Extrapolation procedure. Because computations at very fine resolution are expensive we use linear extrapolation to approximate the ignition-decay boundary. In the example of figure 7(a) intermediately fine partitions with $h_x = 0.01$ and $h_x = 0.005$ are used to determine two points on the upper boundary and two points on the lower boundary of the "frozen" region by DNS. These points are then linearly extrapolated up to their intersection point, as follows.

```
# linear extrapolation
fu:=x->a*x+b: equ1:=yu1=fu(hx1): equ2:=yu2=fu(hx2):
fl:=x->A*x+B: eql1:=yl1=fl(hx1): eql2:=yl2=fl(hx2):
EQ:=fu(hxi)=fl(hxi):
solve({equ1,equ2,eql1,eql2,EQ},{a,b,A,B,hxi}):
```

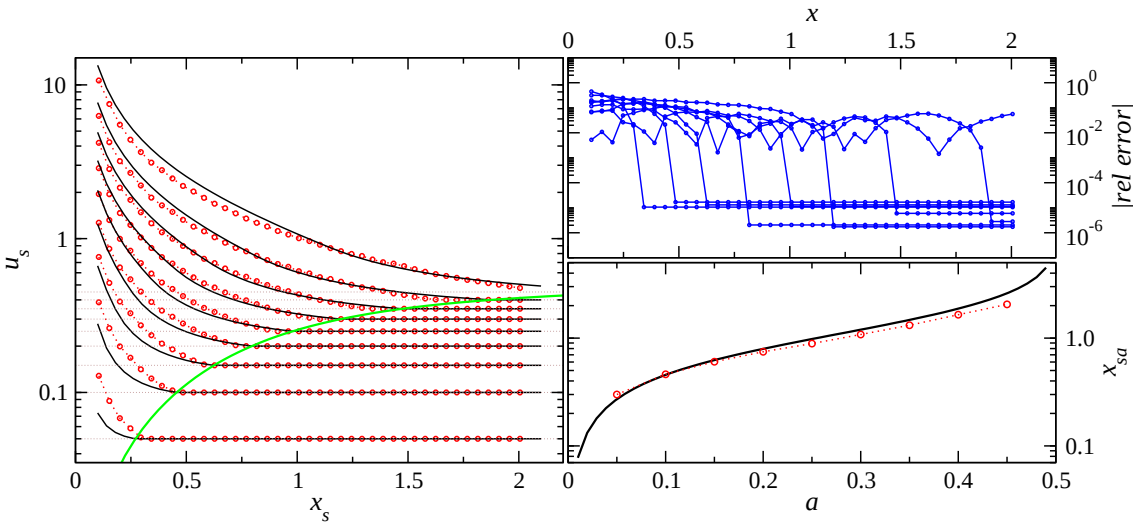

Figure 8: (a) Strength-extent curves $u_s(x_s)$ – comparison of the analytical approximation formula (32) (black solid lines) with results from direct numerical simulations (red circles on dotted lines). The values of a increase from bottom at 0.05 to top at 0.45 by 0.05. (b) The absolute value of the relative error between direct numerical simulations and the analytical approximation formula for the strength-extent curves for the same cases shown in (a). (c) The minimal distance x_{sa} above which voltage of amplitude $u_s = a$ or greater causes ignition – comparison of the analytical approximation formula (31) (black solid line) with results from direct numerical simulations (red circles on a dotted line). There is no excitation if $u_s < a$, no matter how large the support x_s is. The same curve is given in green in panel (a).

```
assign(%):

lprint(simplify(hxi));
lprint(simplify(fu(hxi)));

hx1:= 0.01000000: yu1:=2.15834638: yl1:=2.10565804:
hx2:= 0.00500000: yu2:=2.15407442: yl2:=2.13021041:
hxi:=simplify(hxi); yi:=simplify(fu(hxi));
fu(x);
fl(x);
```

giving

```
-(-hx1*yu2+hx1*yl2+yu1*hx2-yl1*hx2)/(-yu1+yu2+yl1-yl2)
(-yu1*yl2+yu2*yl1)/(-yu1+yu2+yl1-yl2)
hxi := 0.0008604397743 ; yi := 2.150537613
0.8543920000 x + 2.149802460
-4.910474000 x + 2.154762780
```

4.3 Comparison of analytical approximation and DNS

4.3.1 Initiation by voltage: strength-extent curve

Comparison of analytical approximation for the strength-extent curve (32) and DNS is shown in figure 8. Remarkably good agreement is found over the entire parameter range of a. Indeed, the modulus of the local relative error

$$|\text{rel error}(x_s)| = \left| \frac{\Big[u_s(x_s)\Big]_{\text{DNS}} - \Big[u_s(x_s)\Big]_{\text{f-la (32)}}}{u_s(x_s)|_{\text{DNS}}} \right|, \tag{36}$$

between the direct numerical simulations and the analytical approximation formula for the strength-extent curves is plotted in figure 8(b) for the all corresponding cases from figure 8(a). In all cases the relative error is of the order of 10%.

4.3.2 Initiation by current: strength-duration curve

PROBLEM - RDS found a huge discrepancy when comparing the analytical approximation for the strength-extent curve (33) to DNS but no obvious error. RDS needs to think.

5 Travelling wave solutions

5.1 Analytical

Reported by Rinzel and Keller [13].

5.2 Numerical

5.2.1 DNS

5.2.2 Sturm-Liouville eigenvalue problem for wave speed c

The problem can be solved in the same way as [14, 15] where we have successfully treated more complicated problems.

Part II
Fronts in Beeler-Reuter model – Example of a critical moving front (travelling wave)

6 Introduction

Certain problems do not have standing wave solutions, i.e. critical nucleus solutions as defined in Definition 1. Instead, some problems have travelling wave solutions, i.e. solutions of fixed shape travelling at constant non-zero speed c, and [6] propose that an unstable travelling wave solution plays the same role as the critical nucleus in our theory of front initiation. Examples of models that do not have standing wave solutions are, in increasing order of complexity, (a) the Biktashev front model [3] (analytical solution possible); (b) the Caricature Noble model of [4, 15] (analytical solution possible); (c) Beeler-Reuter model (analytical solution not possible because of $\tau_h(V)$). Here we consider the Beeler-Reuter model [2] as an example of fairly realistic complexity. The analysis is done numerically.

7 The Beeler-Reuter model

7.1 The authentic model

We rewrite the authentic Beeler-Reuter model [2] in the one-parameter form,

$$\frac{\partial E}{\partial t} = \frac{1}{\epsilon} g_{\mathrm{Na}} \left(E_{\mathrm{Na}} - E\right) \underline{m_\infty}(E;\epsilon)\, j\, h + I_\Sigma(E,\mathbf{y}) + \epsilon \frac{\partial^2 E}{\partial x^2}, \tag{37a}$$

$$\frac{\partial h}{\partial t} = \frac{1}{\epsilon}\big(\underline{h_\infty}(E;\epsilon) - h\big)/\tau_h(E), \tag{37b}$$

$$\frac{\partial j}{\partial t} = \big(j_\infty(E) - j\big)/\tau_j(E) \tag{37c}$$

$$\frac{\partial \mathbf{y}}{\partial t} = \mathbf{F}_{\mathbf{y}}(E,\mathbf{y},\dots), \tag{37d}$$

with $\underline{m_\infty}(E;0) = \theta(E - E_m)$ and $\underline{h_\infty}(E;0) = \theta(E_h - E)$, where only the equations affected by the artificial small parameter $\epsilon \ll 1$ are shown.

7.2 Travelling wave ansatz

We look for "travelling wave" solutions. Several choices for a travelling wave ansatz are possible and this make difference in the equations and the BCs. Here we use the following change of

variables that describe a wave travelling from left ($-\infty$) to right (∞)

$$z = x - c\,t, \tag{38a}$$
$$s = t. \tag{38b}$$

The corresponding derivative transformation is

$$\frac{\partial}{\partial x} = \frac{\partial}{\partial z}\frac{\partial z}{\partial x} + \frac{\partial}{\partial s}\frac{\partial s}{\partial x} = \frac{\partial}{\partial z}, \qquad \frac{\partial^2}{\partial x^2} = \frac{\partial^2}{\partial z^2}, \tag{39a}$$
$$\frac{\partial}{\partial t} = \frac{\partial}{\partial z}\frac{\partial z}{\partial t} + \frac{\partial}{\partial s}\frac{\partial s}{\partial t} = -c\frac{\partial}{\partial z} + \frac{\partial}{\partial s} = -c\frac{\partial}{\partial z}. \tag{39b}$$

Above ∂_s is set to zero because s corresponds to time and we look for travelling wave of "fixed shape", i.e. solutions where there is no other time-variation apart from translation. Translation is captured by the speed c.

With this Beeler-Reuter model (37) becomes

$$-c\frac{\partial E}{\partial z} = \frac{1}{\epsilon} g_{\mathrm{Na}}\,(E_{\mathrm{Na}} - E)\,\underline{m_\infty}(E;\epsilon)\,j\,h + I_\Sigma(E,\mathbf{y}) + \epsilon\frac{\partial^2 E}{\partial z^2}, \tag{40a}$$
$$-c\frac{\partial h}{\partial z} = \frac{1}{\epsilon}\big(\underline{h_\infty}(E;\epsilon) - h\big)/\tau_h(E), \tag{40b}$$
$$-c\frac{\partial j}{\partial z} = \big(j_\infty(E) - j\big)/\tau_j(E) \tag{40c}$$
$$-c\frac{\partial \mathbf{y}}{\partial z} = \mathbf{F}_{\mathbf{y}}(E,\mathbf{y},\dots). \tag{40d}$$

8 Critical front of the Beeler-Reuter model

8.1 Front in the Beeler-Reuter model

The travelling front is the solution of the fast-time subsystem of the authentic Beeler-Reuter equations (40). The fast-time system is derived by a Non-Tichonov asymptotic embedding in section 7 of [15]. Rescale the travelling wave coordinate

$$Z = z/\epsilon, \qquad \frac{\partial}{\partial z} = \frac{1}{\epsilon}\frac{\partial}{\partial Z}, \quad \frac{\partial^2}{\partial z^2} = \frac{1}{\epsilon^2}\frac{\partial^2}{\partial Z^2}.$$

Multiply by ϵ throughout. Take the limit $\epsilon \to 0^+$. The $\mathbf{y}$ equation decouples and we get the fast-time subsystem

$$\frac{\mathrm{d}^2 V}{\mathrm{d}Z^2} = -c\frac{\mathrm{d}V}{\mathrm{d}Z} - g_{\mathrm{Na}}(E_{\mathrm{Na}} - V)\,J\,\theta(V - E_m)\,H, \tag{41a}$$
$$\frac{\mathrm{d}H}{\mathrm{d}Z} = -\frac{1}{c}\frac{1}{\tau_h(V)}\Big(\theta(E_h - V) - H\Big). \tag{41b}$$

In terms of an equivalent first-order system

$$V' = U, \tag{42a}$$
$$U' = -cU - g_{\mathrm{Na}}(E_{\mathrm{Na}} - V)\,J\,\theta(V - E_m)\,H, \tag{42b}$$
$$H' = -\frac{1}{c}\frac{1}{\tau_h(V)}\Big(\theta(E_h - V) - H\Big). \tag{42c}$$

A typical solution is shown in fig. 9. The figure illustrates typical features and is a useful picture to have in mind when setting the eigen-boundary value problem in the next section.

8.1.1 Partitioning

Partition the domain of integration $Z \in (-\infty, Z_m] \cup [Z_m, 0] \cup [0, \infty)$ as shown in fig. 9. Denote all quantities on interval $(-\infty, Z_m]$ by index $(_{:1})$, all quantities on interval $[Z_m, 0]$ by index $(_{:2})$ and all quantities on interval $[0, \infty)$ by index $(_{:3})$. On these intervals the equations take the form,

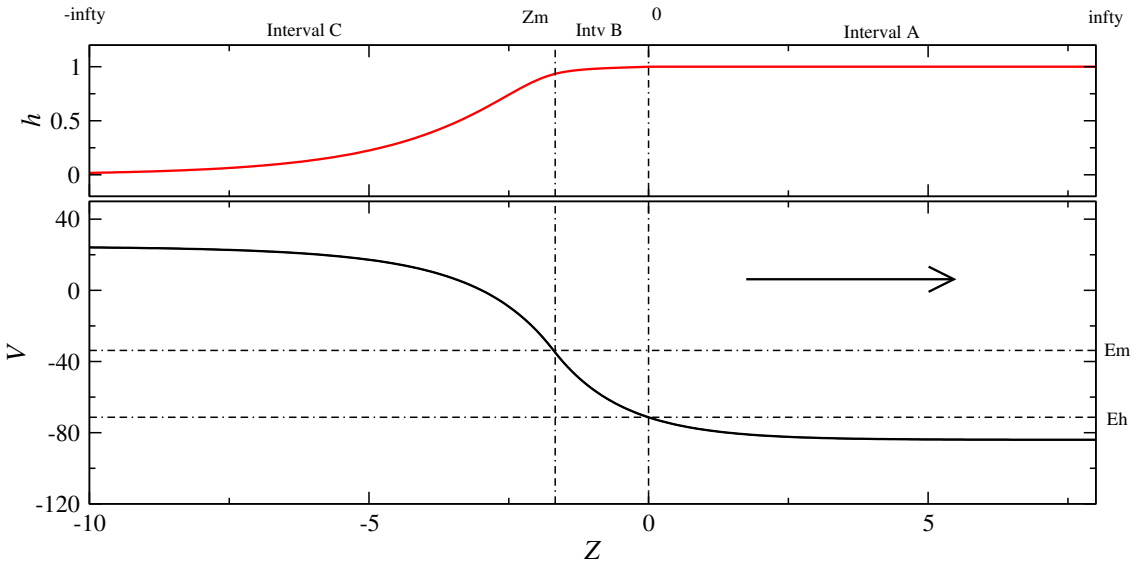

Figure 9:

$$
\begin{aligned}
&Z_{:1} \in (-\infty, Z_m],\\
&V_{:1} \in [E_m, \infty),\\
&\theta(V_{:1} - E_m) = 1,\\
&\theta(E_h - V_{:1}) = 0,\\
&-\,-\,-\,-\,-\,-\,-\\
&V_{:1}{}' = U_{:1},\\
&U_{:1}{}' = -cU_{:1} - g_{\mathrm{Na}}(E_{\mathrm{Na}} - V_{:1})\, J\, H_{:1},\\
&H' = -\frac{(-H_{:1})}{c\tau_h(V_{:1})}.
\end{aligned}
\tag{43}
$$

$$
\begin{aligned}
&Z_{:2} \in [Z_m, 0],\\
&V_{:2} \in [E_h, E_m],\\
&\theta(V_{:2} - E_m) = 0,\\
&\theta(E_h - V_{:2}) = 0,\\
&-\,-\,-\,-\,-\,-\,-\\
&V_{:2}{}' = U_{:2},\\
&U_{:2}{}' = -cU_{:2},\\
&H_{:2}{}' = -\frac{(-H_{:2})}{c\tau_h(V_{:2})}.
\end{aligned}
\tag{44}
$$

$$
\begin{aligned}
&Z_{:3} \in [0, \infty),\\
&V_{:3} \in [E_h, -\infty),\\
&\theta(V_{:3} - E_m) = 0,\\
&\theta(E_h - V_{:3}) = 1,\\
&-\,-\,-\,-\,-\,-\,-\\
&V_{:3}{}' = U_{:3},\\
&U_{:3}{}' = -cU_{:3},\\
&H_{:3}{}' = -\frac{(1-H_{:3})}{c\tau_h(V_{:3})}.
\end{aligned}
\tag{45}
$$

8.2 Boundary Conditions

8.2.1 Spatially uniform equilibrium states

A travelling front in a bistable system such as (42) is a "zipping" transition between two stable spatially uniform equilibria. These equilibria serve as boundary conditions for the problem at infinity. We find the equilibria as the roots of the RHS of (42) i.e.

$$
\begin{aligned}
&U = 0, && \text{(46a)}\\
&-cU - g_{\mathrm{Na}}(E_{\mathrm{Na}} - V)\, J\, \theta(V - E_m)\, H = 0, && \text{(46b)}\\
&-\frac{1}{c}\frac{1}{\tau_h(V)}\Big(\theta(E_h - V) - H\Big) = 0, && \text{(46c)}
\end{aligned}
$$

and these are

$$
\begin{aligned}
&\text{Equilibrium at } \infty: && (V, U, H)_{\infty} = (V_\alpha < E_h, 0, 1), && \text{(47a)}\\
&\text{Equilibrium at } -\infty: && (V, U, H)_{-\infty} = (V_\omega > E_m, 0, 0), && \text{(47b)}\\
& && && \text{(47c)}
\end{aligned}
$$

where V_α and V_ω are arbitrary constants in the specified ranges.

8.2.2 Boundary conditions

So we require the boundary conditions

$$
\begin{aligned}
&V(\infty) = V_\alpha, \quad V'(\infty) = 0, \quad H(\infty) = 1, && \text{(48a)}\\
&V(-\infty) = V_\omega, \quad V'(-\infty) = 0, \quad H(-\infty) = 0, && \text{(48b)}\\
&V(0) = E_h. && \text{(48c)}
\end{aligned}
$$

The last equation is a "phase condition" for fixing c.

Degrees of freedom check: 3rd order system plus 3 unknowns, c, V_α, and V_ω gives 6 degrees of freedom and we have 7 constraints. So it would the system is overdetermined and will not have any solution! This however, is not so because these are asymptotic relations and not strict, and a more careful analysis reveals additional degrees of freedom.

8.2.3 Boundary Asymptotics

Consider small perturbations about the equilibria. At $-\infty$

$$\begin{aligned} V_{:1} &= E_\omega + \tilde{V}_{:1}, \quad O(\tilde{V}_{:1}) \ll 1, \\ U_{:1} &= 0 + \tilde{U}_{:1}, \quad O(\tilde{U}_{:1}) \ll 1, \\ H_{:1} &= 1 + \tilde{H}_{:1}, \quad O(\tilde{H}_{:1}) \ll 1, \end{aligned}$$

Linearise the first-order system (43)

$$\begin{bmatrix} \tilde{V}_{:1}{}' \\ \tilde{U}_{:1}{}' \\ \tilde{H}_{:1}{}' \end{bmatrix} = \begin{bmatrix} 0 & 1 & 0 \\ 0 & -c & -g_{\mathrm{Na}}(E_{\mathrm{Na}} - E_\omega)\, J \\ 0 & 0 & 1/(c\tau_h(E_\omega)) \end{bmatrix} \begin{bmatrix} \tilde{V}_{:1} \\ \tilde{U}_{:1} \\ \tilde{H}_{:1} \end{bmatrix},$$

Write the solutions with the help of the eigenvalues and eigenvectors of the coefficient matrix

$$\begin{bmatrix} \tilde{V}_{:1} \\ \tilde{U}_{:1} \\ \tilde{H}_{:1} \end{bmatrix} = \begin{bmatrix} 1 & -\frac{1}{c} & -\frac{g_{\mathrm{Na}}(E_{\mathrm{Na}} - E_\omega)Jc^2\tau_h(E_\omega)^2}{(c^2\tau_h(E_\omega)+1)} \\ 0 & 1 & -\frac{g_{\mathrm{Na}}(E_{\mathrm{Na}} - E_\omega)Jc\tau_h(E_\omega)}{(c^2\tau_h(E_\omega)+1)} \\ 0 & 0 & 1 \end{bmatrix} \begin{bmatrix} C_1 \exp(0 Z_{:1}) \\ C_2 \exp(-c Z_{:1}) \\ C_3 \exp\left(\dfrac{Z_{:1}}{c\tau_h(E_\omega)}\right) \end{bmatrix}.$$

Since the perturbations must remain small as $Z_{:1} \to -\infty$ we require that the coefficients at the non-positive eigenvalues vanish $C_1 = 0$, $C_2 = 0$ so the equilibrium is linearly stable, then

$$\begin{bmatrix} \tilde{V}_{:1} \\ \tilde{U}_{:1} \\ \tilde{H}_{:1} \end{bmatrix} = \begin{bmatrix} 1 & -\frac{1}{c} & -\frac{g_{\mathrm{Na}}(E_{\mathrm{Na}} - E_\omega)Jc^2\tau_h(E_\omega)^2}{(c^2\tau_h(E_\omega)+1)} \\ 0 & 1 & -\frac{g_{\mathrm{Na}}(E_{\mathrm{Na}} - E_\omega)Jc\tau_h(E_\omega)}{(c^2\tau_h(E_\omega)+1)} \\ 0 & 0 & 1 \end{bmatrix} \begin{bmatrix} 0 \\ 0 \\ C_3 \exp\left(\dfrac{Z_{:1}}{c\tau_h(E_\omega)}\right) \end{bmatrix}.$$

Thus the boundary conditions at $-\infty$ are

$$V_{:1} = E_\omega - C_3 \frac{g_{\mathrm{Na}}(E_{\mathrm{Na}} - E_\omega)Jc^2\tau_h(E_\omega)^2}{(c^2\tau_h(E_\omega)+1)} \exp\left(\frac{Z_{:1}}{c\tau_h(E_\omega)}\right) \quad \text{as} \quad Z_{:1} \to -\infty, \tag{49}$$

$$U_{:1} = -C_3 \frac{g_{\mathrm{Na}}(E_{\mathrm{Na}} - E_\omega)Jc\tau_h(E_\omega)}{(c^2\tau_h(E_\omega)+1)} \exp\left(\frac{Z_{:1}}{c\tau_h(E_\omega)}\right) \quad \text{as} \quad Z_{:1} \to -\infty, \tag{50}$$

$$H_{:1} = C_3 \exp\left(\frac{Z_{:1}}{c\tau_h(E_\omega)}\right) \quad \text{as} \quad Z_{:1} \to -\infty. \tag{51}$$

Similar analysis at $Z_{:3} \to \infty$. We take

$$\begin{aligned} V_{:3} &= E_\alpha + \tilde{V}_{:3}, \quad O(\tilde{V}_{:3}) \ll 1, \\ U_{:3} &= 0 + \tilde{U}_{:3}, \quad O(\tilde{U}_{:3}) \ll 1, \\ H_{:3} &= 1 + \tilde{H}_{:3}, \quad O(\tilde{H}_{:3}) \ll 1. \end{aligned}$$

Then linearize (45)

$$\begin{bmatrix} \tilde{V}_{:3}{}' \\ \tilde{U}_{:3}{}' \\ \tilde{H}_{:3}{}' \end{bmatrix} = \begin{bmatrix} 0 & 1 & 0 \\ 0 & -c & 0 \\ 0 & 0 & 1/(c\tau_h(E_\alpha)) \end{bmatrix} \begin{bmatrix} \tilde{V}_{:3} \\ \tilde{U}_{:3} \\ \tilde{H}_{:3} \end{bmatrix}.$$

Write the solutions with the help of the eigenvalues and eigenvectors of the coefficient matrix

$$\begin{bmatrix} \tilde{V}_{:3} \\ \tilde{U}_{:3} \\ \tilde{H}_{:3} \end{bmatrix} = \begin{bmatrix} 1 & -1/c & 0 \\ 0 & 1 & 0 \\ 0 & 0 & 1 \end{bmatrix} \begin{bmatrix} C_4 \exp(0 Z_{:1}) \\ C_5 \exp(-c Z_{:1}) \\ C_6 \exp\left(\dfrac{Z_{:1}}{c\tau_h(E_\alpha)}\right) \end{bmatrix}.$$

Since the perturbations must remain small as $Z_{:3} \to \infty$ we require that the coefficients at the non-negative eigenvalues vanish $C_4 = 0$, $C_6 = 0$ so the equilibrium is linearly stable, then

$$\begin{bmatrix} \tilde{V_{:3}} \\ \tilde{U_{:3}} \\ \tilde{H_{:3}} \end{bmatrix} = \begin{bmatrix} 1 & -1/c & 0 \\ 0 & 1 & 0 \\ 0 & 0 & 1 \end{bmatrix} \begin{bmatrix} 0 \\ C_5 \exp(-cZ_{:3}) \\ 0 \end{bmatrix}.$$

Thus the boundary conditions at ∞ are

$$V_{:3} = E_\alpha - C_5 \frac{1}{c} \exp(-cZ_{:3}) \quad \text{as } Z_{:3} \to \infty, \tag{52}$$

$$U_{:3} = C_5 \exp(-cZ_{:3}) \quad \text{as } Z_{:3} \to \infty, \tag{53}$$

$$H_{:3} = 1 \quad \text{as } Z_{:3} \to \infty. \tag{54}$$

/rswork1/02_Papers_Proposals/017_InitiationofExcitation/02Calcs/0704_BeelerReuter/000_Formulation/010LinearApproxBC-infty.M
/rswork1/02_Papers_Proposals/017_InitiationofExcitation/02Calcs/0704_BeelerReuter/000_Formulation/010LinearApproxBC+infty.M

We now have our degrees of freedom check again. We have introduced 2 new unknown parameters - C_3 and C_5. So 3rd order system plus 5 unknowns, c, V_α, V_ω C_3 and C_5 gives 8 degrees of freedom and we have 7 constraints. So a BVP with one-parameter family of solutions.

8.3 Replace the infinite domain of integration by finite

This is now trivial after the work done in the previous section. The asymptotic BCs (49) and (52) remain valid for sufficiently large but finite interval.

8.4 Map the domains of integration to [0,1]

We define the following maps and find the following derivative transformations

$$Z_{:3} \in [0, l] \to [0, 1] \ni \underset{\sim}{x} \quad \text{by} \quad \underset{\sim}{x} = \frac{Z_{:3}}{l} \qquad \Rightarrow \qquad \frac{\partial}{\partial Z_{:3}} = \frac{1}{l} \frac{\partial}{\partial Z_{:3}}, \tag{55}$$

$$Z_{:2} \in [Z_m, 0] = [-l/|p|, 0] \to [1, 0] \ni \underset{\sim}{x} \quad \text{by} \quad \underset{\sim}{x} = -\frac{|p|}{l} Z_{:2} \qquad \Rightarrow \qquad \frac{\partial}{\partial Z_{:2}} = -\frac{|p|}{l} \frac{\partial}{\partial \underset{\sim}{x}}, \tag{56}$$

$$Z_{:1} \in [-l + Z_m, Z_m] = [-l - \frac{l}{|p|}, -\frac{l}{|p|}] \to [0, 1] \ni \underset{\sim}{x} \quad \text{by} \quad \underset{\sim}{x} = -\frac{Z_{:1}}{l} - |p| \qquad \Rightarrow \qquad \frac{\partial}{\partial Z_{:2}} = -\frac{1}{l} \frac{\partial}{\partial \underset{\sim}{x}}. \tag{57}$$

This remapping looks somewhat strange with the arbitrary scaling $|p|$ and mirror reflections in the y-axis, but I keep it for historical reasons.

8.5 Summary of the BVP and numerical implementation and solution

Using change of variables (55), the equations (43,43,43) and the BCs (49,52) take the final form

$$\begin{aligned}
V_{:3}{}' &= l U_{:3}, \\
U_{:3}{}' &= l\Big(- c U_{:3} \Big), \\
H_{:3}{}' &= l\Big(- \frac{(1 - H_{:3})}{c \tau_h(V_{:3})} \Big), \\
&- - - - - - \\
V_{:2}{}' &= (-\frac{l}{|p|}) U_{:2}, \\
U_{:2}{}' &= (-\frac{l}{|p|}) \Big(- c U_{:2} \Big), \\
H_{:2}{}' &= (-\frac{l}{|p|}) \Big(- \frac{(-H_{:2})}{c \tau_h(V_{:2})} \Big), \\
&- - - - - - \\
V_{:1}{}' &= (-l) U_{:1}, \\
U_{:1}{}' &= (-l) \Big(- c U_{:1} - g_{\mathrm{Na}} (E_{\mathrm{Na}} - V_{:1})\, J\, H_{:1} \Big), \\
H' &= (-l) \Big(- \frac{(-H_{:1})}{c \tau_h(V_{:1})} \Big).
\end{aligned} \tag{58, 59, 60}$$

$$
\begin{aligned}
V_{:1}(0) &= E_h \\
V_{:2}(0) &= E_h \\
V_{:3}(0) &= E_m \\
U_{:1}(0) &= U_{:2}(0) \\
H_{:1}(0) &= H_{:2}(0) \\
U_{:3}(0) &= U_{:2}(1) \\
H_{:1}(0) &= H_{:2}(1) \\
U_{:1}(1) &= -c(V_{:1}(1) - E_\alpha) \\
V_{:2}(1) &= E_m \\
U_{:3}(1) &= (V_{:3}(1) - E_\omega)/c/\tau_h(V_{:3}(1)) \\
H_{:1}(1) &= 1 \\
H_{:3}(1) &= -U_{:3}(1)/g_{\mathrm{Na}}/J/(E_{\mathrm{Na}} - E_\omega)(1/c/\tau_h(E_\omega) + c)
\end{aligned}
\tag{61}
$$

In that formulation we eliminate the unknown constants C_3 and C_5 from (49,52) to avoid providing initial estimates for them.

The MAPLE code for the problem is just the same as the equations above.

```
#############################################################################
NumbEqus:=9:
NumbBCs:=12:  # + 3 unknown params

#...The Equations that we need to solve, formulated as a first order system
#-----------------------------3--------------------------
 F[1] := diff(E3(z),z)     = l*(Eprim3(z)):
 F[2] := diff(Eprim3(z),z) = l*(-c*Eprim3(z)):
 F[3] := diff(h3(z),z)     = l*(-1/c/th(E3(z))*(1-h3(z))):
#-----------------------------2--------------------------
 F[4] := diff(E2(z),z)     = (-l/p)*Eprim2(z):
 F[5] := diff(Eprim2(z),z) = (-l/p)*(-c*Eprim2(z)):
 F[6] := diff(h2(z),z)     = (-l/p)*(-1/c/th(E2(z))*(-h2(z))):
#-----------------------------1--------------------------
 F[7] := diff(E1(z),z)     = (-l)*Eprim1(z):
 F[8] := diff(Eprim1(z),z) = (-l)*(-c*Eprim1(z) -gNa*jalpha*(eNa-E1(z))*h1(z)):
 F[9] := diff(h1(z),z)     = (-l)*(-1/c/th(E1(z))*(-h1(z))):
#-------------------------------------------------------

#The boundary conditions in the format of the D02RAF are
 AL[1] := E3(0)      = Vh:
 AL[2] := E2(0)      = Vh:
 AL[3] := E1(0)      = Vm:
 AL[4] := Eprim3(0)  = Eprim2(0):
 AL[5] := h3(0)      = h2(0):
 AL[6] := Eprim1(0)  = Eprim2(1):
 AL[7] := h1(0)      = h2(1):
 AL[8] := Eprim3(1)  = -c*(E3(1)-Ealpha):
 AL[9] := E2(1)      = Vm:
 AL[10] := Eprim1(1) = (E1(1)-Eomega)/c/th(E1(1)):
 AL[11] := h3(1)     = 1:
 AL[12] := h1(1)     = -Eprim1(1)/gNa/jalpha/(eNa-Eomega)*(1/c/th(Eomega)+c):

#--- constants
eNa := 50.:
eK  := -85:
gNa := 4.:
gK  := 0.35:
Vm:=-33.75:
Vh:=-71.33:

l:=10:

BVPROBLEM:=[seq(F[i],i=1..NumbEqus), seq(AL[i],i=1..NumbBCs)]:

th:=proc(V)
```

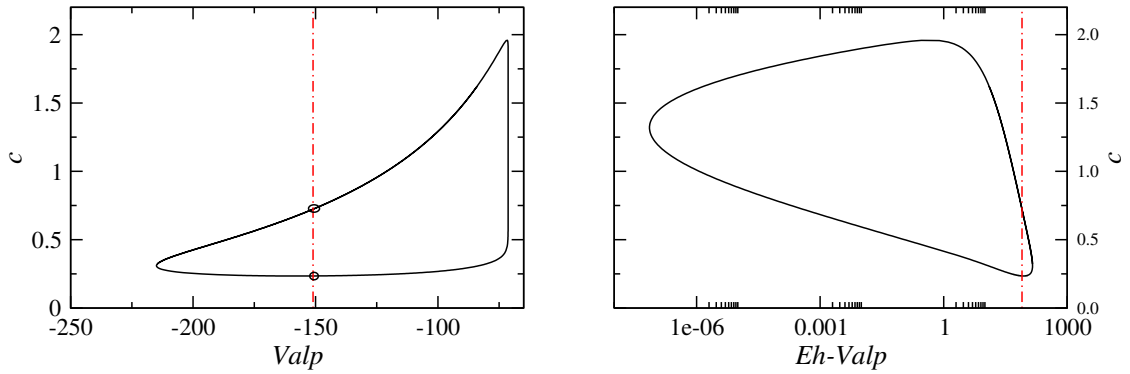

Figure 10: $J = 0.8$ The vertical line indicates the location of the stable and the unstable solutions plotted in fig. 11

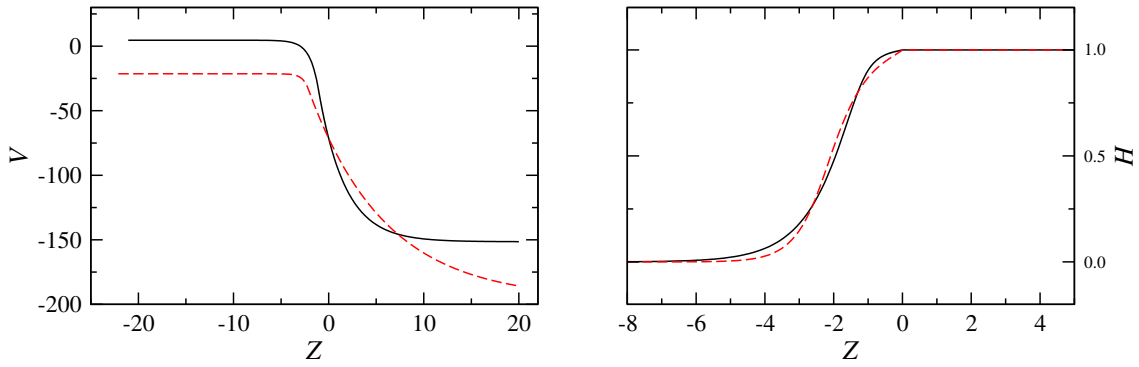

Figure 11: A stable (black solid lines) and an unstable (red broken lines) solutions with $E_\alpha = -151$. $J = 0.8$

```
 local ah, bh:
 ah := (0.1260*exp(-0.250*(V+77.))):
 bh := 1.7/(exp(-0.082*(V+22.5))+1.):
 1./(ah+bh);
end proc:
################################################
```

/rswork1/02_Papers_Proposals/017_InitiationofExcitation/02Calcs/0704_BeelerReuter/010CriticalFastFront/2015-03-24/02FastEqns.M

The equations are then solved using the MAPLE `dsolve,numeric` command.

```
################################################
dynvars:=[E3(z),E2(z),E1(z),Eprim3(z),Eprim2(z),Eprim1(z),h3(z),h2(z),h1(z)]:
solopts:=method=bvp[middefer],'range'=0..1,'approxsoln'=Ybvp,
                        maxmesh=8192,'abserr'=Float(1,-5),'optimize'=true,output=mesh:

Ybvp:= dsolve(BVPROBLEM,numeric,dynvars,solopts):
################################################
```

To trace the solution to the unstable braches one needs to do some parameter continuation. The details of how this is done are in the program below and the details are hopefully easy to understand.

/rswork1/02_Papers_Proposals/017_InitiationofExcitation/02Calcs/0704_BeelerReuter/010CriticalFastFront/2015-03-24/00c_BeelerReuter_BVP.M
/rswork1/02_Papers_Proposals/017_InitiationofExcitation/02Calcs/0704_BeelerReuter/010CriticalFastFront/2015-03-24/02FastEqns.M
/rswork1/02_Papers_Proposals/017_InitiationofExcitation/02Calcs/0704_BeelerReuter/010CriticalFastFront/2015-03-24/ServiceProcs.M
/rswork1/02_Papers_Proposals/017_InitiationofExcitation/02Calcs/0704_BeelerReuter/010CriticalFastFront/2015-03-24/11IAc.M

Finally, some plots of the solution. fig. 10 shows a Conduction velocity c as a function of the one free parameter E_α. Continuation in any other parameter, say E_ω, c, p may be done, alternatively. This curve is useful to follow the stable and unstable branches. The unstable branch is the one with smaller c. We fix J, as this plays the role of a excitation of the medium.

fig. 11 shows a stable and an unstable solution.

References

[1] P.B. Bailey, M.K. Gordon, and L.F. Shampine. Automatic solution of the Sturm-Liouville problem. *ACM Trans. Math. Software*, 4:193–207, 1978.

[2] G. W. Beeler and H Reuter. Reconstruction of the action potential of ventricular myocardial fibres. *J. Physiol. Lond.*, 268:177–210, 1977.

[3] V. N. Biktashev. Dissipation of the excitation wavefronts. *Phys. Rev. Lett.*, 89(16):168102, 2002.

[4] V. N. Biktashev, R. S. Suckley, Y. E. Elkin, and R. D. Simitev. Asymptotic analysis and analytical solutions of a model of cardiac excitation. *Bull. Math. Biol.*, 70(2):517–554, 2008.

[5] R. M. Corless, G. H. Gonnet, D. E. G. Hare, D. J. Jeffrey, and D. E. Knuth. On the Lambert W function. *Adv. Comp. Math.*, 5:329–359, 1996.

[6] I. Idris and V. N. Biktashev. Critical fronts in initiation of excitation waves. *Phys. Rev. E*, 76(2):021906, 2007.

[7] I. Idris and V. N. Biktashev. Analytical approach to initiation of propagating fronts. *Physical Review Letters*, 101(24):244101, 2008.

[8] M. Marletta and J.D. Pryce. Automatic solution of Sturm-Liouville prob- lems using the Pruess method. *J. Comput. Appl. Math.*, 39:57–78, 1992.

[9] H. P. McKean. Nagumo's equation. *Adv. Math.*, 4(3):209–223, 1970.

[10] NAG. The Numerical Algorithms Group, Ltd. Fortran Library Manual, Mark 20.

[11] J.D. Pryce. *Numerical Solution of Sturm-Liouville Problems*. Oxford University Press, Oxford, 1993.

[12] J.D. Pryce. A test package for Sturm-Liouville solvers. *ACM Trans. Math. Software*, 25:21–57, 1999.

[13] J. Rinzel and J. Keller. Traveling Wave Solutions of a Nerve Conduction Equation. *Biophysical Journal*, 13(12):1313–1337, 1973.

[14] R. D. Simitev and V. N. Biktashev. Conditions for propagation and block of excitation in an asympthotic model of atrial tissue. *Biophysical Journal*, 90:2258–2269, 2006.

[15] R.D. Simitev and V.N. Biktashev. Asymptotics of conduction velocity restitution in models of electrical excitation in the heart. *Bull. Math. Biol.*, 73(1):72–115, 2011.